


Glass transition in gels

Rui Xiao ^{1,*} and Hai Li²

¹State Key Laboratory of Fluid Power & Mechatronic System,
Key Laboratory of Soft Machines and Smart Devices of Zhejiang Province,
Department of Engineering Mechanics, Zhejiang University, Hangzhou 310027, China

²Department of Engineering Mechanics, College of Mechanics and Materials,
Hohai University, Nanjing, Jiangsu 210098, China



(Received 28 February 2021; revised 21 April 2021; accepted 8 June 2021; published 21 June 2021)

Recent works have shown that gels with a large amount of solvents can still exhibit a glass transition behavior with the thermomechanical properties exhibiting tremendous change over a narrow temperature region. Similar to dry polymers, the rheological behaviors of gels also show a broad distribution of relaxation times. However, so far the effects of solvents on the relaxation spectrum have rarely been studied. In this work, we first develop a viscoelastic model to relate the rheological properties of gels and the corresponding properties in the dry state. We then apply the theoretical model to analyze the complex modulus of gels measured in the small strain dynamic tests. The results show that the breadth of relaxation spectrum has been expanded by increasing the swelling ratio. The physical mechanism behind this observation needs a deep investigation in further study and also raises a significant challenge for developing constitutive models for gels.

DOI: [10.1103/PhysRevMaterials.5.065604](https://doi.org/10.1103/PhysRevMaterials.5.065604)

I. INTRODUCTION

Glass transition has been widely observed in various materials systems, ranging from amorphous solids, colloidal suspensions, supercooled liquids, granular materials, etc. [1–3]. Across the glass transition region, the properties, such as heat capacity, dielectric constant, refraction index, modulus, and viscosity, show a tremendous change even by many orders of magnitudes [4,5]. So far a general theory for glass transition is still far from settled, though several theories like the classic configurational entropy theory [6,7], mode-coupling theory [8,9], and more recently random first order transition theory [10] can illustrate many important features of glass transition. In addition, Zaccane and Terentjev [11] developed a theory for glass transition in solids, which shows that the sharp drop of shear modulus across the glass transition region of polymers is controlled by nonaffine displacements and their interplay with thermal expansion. This theoretical framework can provide an excellent parameter-free description on the frequency-dependent storage modulus and loss modulus of amorphous polymers [12]. Najafi *et al.* [13] successfully applied the above theory to describe the dependence of the modulus of microgels on the effective volume fraction. These works can provide insight on the physical origin of glass transition.

Gels, composed of chemically cross-linked polymer networks and solvents, are ubiquitous in our daily life. However, different from dry polymers, the glass transition behaviors of gels have been rarely studied in the literature. In fact, gels are commonly assumed to be elastic materials [14,15], though

several works [16–21] have also reported the rate-dependent viscoelastic response in gels. If gels can exhibit a glass transition behavior, the glass transition temperature (T_g) in gels will be significantly lower than the corresponding dry polymers due to the remarkable plasticization effects. For hydrogels, if the T_g is below the freezing temperature of water, it is typically not possible to observe the glass transition behavior. Instead, a frozen stiff gel with crystallized ice can be obtained [22]. Thus, for hydrogels to demonstrate a glass transition behavior, the T_g of the polymer matrix needs to be well above the freezing temperature of water. For example, Wang *et al.* [23] have reported the T_g of tough hydrogels around 60 °C while the dry polymer has a T_g of 190 °C. In addition to water, it is also possible to use the organic solvents with a low freezing point to swell gels. For example, Xiao *et al.* [24] showed that the glass transition temperature of a gel system composed of acrylate polymers and isopropyl alcohol (IPA) can be tuned from 40 °C to –50 °C through controlling the amount of IPA, which has a freezing point of –90 °C.

So far, the research on glass transition behaviors of gels is still in its infancy. Several fundamental issues remain unsolved. For example, the viscoelastic relaxation behaviors of polymers can span multiple decades of time, which means a relaxation spectrum is needed to capture the mechanical response. Polymers typically exhibit a broad distribution in the molecular weight, length of polymer chains, etc., which further results in different time scales for relaxation processes. The recent experimental works [23,25] have also confirmed that the rheological properties of gels also have a broad distribution of relaxation time. For example, the master curve of storage modulus of P(MAAm-co-MAAc) hydrogels can span four to five decades in the frequency domain [23]. In addition to experiments, several groups have also developed models to

*rxiao@zju.edu.cn

describe the viscoelastic behaviors of gels [20,26]. Bosnjak *et al.* [20] developed a model which is able to describe the viscoelastic of VHB elastomers as well as the hyperelastic behaviors of swollen elastomers. Drozdov *et al.* [26] developed a viscoplastic model to describe the mechanical response of HEMA gels with different swelling ratio. However, to the best of our knowledge, no theoretical and experimental works have been carried to investigate the effects of solvents on the distribution of relaxation processes. In order to address the above issue, the rheological properties, such as storage modulus and loss modulus, should be fully characterized for gels with different amounts of solvent concentration. In addition, a theoretical framework should be built to relate the rheological properties of gels with the corresponding properties of dry polymers. This is essential to obtain the intrinsic effect of solvent on the distribution of relaxation processes in polymer matrix.

The paper is arranged as follows. Section II shows the experimental procedures to obtain the dynamic properties of gels with different swelling ratio. A theoretical model is further developed to relate the mechanical properties of gels with those in the dry state in Sec. III. Through combination of the experimental characterization and theoretical model, in Sec. IV we can reveal the change of the mechanical properties, such as modulus and relaxation spectrum, in the presence of solvents. The last section summarizes the main conclusions.

II. EXPERIMENTAL METHODS

Here we investigate the glass transition behaviors of gels. The acrylate-based polymers were synthesized based on the procedures shown in Xiao *et al.* [24]. In brief, the chemicals tert-butyl acrylate (tBA), poly(ethylene glycol) dimethacrylate with molecular weight 550 (PEGDMA), 2, 2-dimethoxy-2-phenylacetophenone (DMPA) and IPA were all ordered from Sigma Aldrich. The polymer solution was obtained through mixing the monomer tBA, the cross-linker PEGDMA and the photoinitiator DMPA with the weight ratio 98:2:0.1 or 80:20:0.1. The polymer solution was injected into two glass slides separated by 1 mm. The curing was achieved in a UV oven (CL-1000L Crosslinker) for 30 mins. The synthesized polymer film was then cut into a size of 20 mm × 5 mm × 1 mm. After immersed in IPA for a different amount of time, the specimens were wrapped by an aluminum foil for 72 hours to achieve a homogeneous solvent distribution. The mechanical characterization was then performed on a DMA Q800 using the dynamic frequency sweep mode. In the tests, the temperature was first increased by 5 °C in a discrete manner from low temperatures to high temperatures and then a dynamic loading with frequencies 0.3 Hz, 1 Hz, 3 Hz, 10 Hz, and 30 Hz was applied to obtain the storage and loss modulus.

III. THEORY

Here we present a constitutive model for the polymer-solvent systems. Since we only focus on the uniaxial deformation conditions, the model is formulated in the principal directions without using complex tensor forms. The polymer is subject to a deformation in the three principal directions with the stretch ratio as λ_i ($i = 1:3$). The stretch ratio

can be caused by either swelling or mechanical deformation leading to a decomposition as $\lambda_i = \lambda_s \lambda_{mi}$, where λ_s is the isotropic stretch ratio caused by swelling and λ_{mi} is stretch ratio caused by mechanical deformation in each principal direction. Due to the broad distribution of relaxation mechanisms, the deformation gradient can also be split into multiple pairs of elastic and viscous parts as $\lambda_i = \lambda_{ji}^e \lambda_{ji}^v$, $j = 1 : N$. The free energy density of the polymer-solvent systems (Ψ) can be represented as [21,27–30]

$$\begin{aligned} \Psi = & \frac{k_B T}{\Omega \phi} ((1 - \phi) \ln(1 - \phi) + \chi \phi(1 - \phi)) \\ & + \frac{G^{\text{eq}}}{2} (\lambda_1^2 + \lambda_2^2 + \lambda_3^2 - 3 - 2 \ln(\lambda_1 \lambda_2 \lambda_3)) \\ & + \sum_j^N \frac{G_j^{\text{neq}}}{2} ((\lambda_{j1}^e)^2 + (\lambda_{j2}^e)^2 + (\lambda_{j3}^e)^2 \\ & - 3 - 2 \ln(\lambda_{j1}^e \lambda_{j2}^e \lambda_{j3}^e)), \end{aligned} \quad (1)$$

where k_B is the Boltzmann's constant, T is the temperature, Ω is the volume per solvent molecule, ϕ is the polymer fraction, G^{eq} is the equilibrium shear modulus, G_j^{neq} is the nonequilibrium shear modulus of the j th relaxation process, and N is the number of relaxation processes. The polymer fraction is related to the total number of the solvent molecule per reference volume of dry polymer (C_s) as $\phi = 1/(1 + \Omega C_s)$. The first term on the right side in Eq. (1) represents the free energy change caused by mixing the polymer and solvent, which has contributions from entropy change and enthalpy change. For this part, the Flory-Huggins model has been adopted, which is described in details in Flory [27] and Hong *et al.* [28]. The second term is the free energy caused by stretching polymer chains, which is a function of the total deformation. The third term is the free energy density caused by the viscoelastic deformation showing dependence on the viscoelastic stretch ratio λ_{ji}^e . This function is similar to the hyperelastic part, which only replaces the total stretch ratio with the viscoelastic stretch ratio. Such an approach is common for constructing the free energy density for the viscoelastic solids [31]. Polymeric materials exhibit rate-dependent viscoelastic responses, such as relaxation and creep. Several molecular-based theories, such as the reptation model [32] and the transient network model [33,34], have been proposed to illustrate the physical mechanism behind the rate-dependent effects in polymers. Here we adopt the rheological phenomenological approach to describe the viscoelastic relaxation since the main focus of work lies on understanding the effects of solvents on the distribution of relaxation processes.

It is typically assumed that the volumetric change is purely caused by swelling, leading to $1 + \Omega C_s - \lambda_1 \lambda_2 \lambda_3 = 0$. Thus, the free energy can be modified by imposing this kinetic constraint as

$$\widehat{\Psi} = \Psi + p(1 + \Omega C_s - \lambda_1 \lambda_2 \lambda_3), \quad (2)$$

where p is a Lagrangian multiplier. Based on thermodynamics, the Cauchy stress σ and the chemical potential μ can be

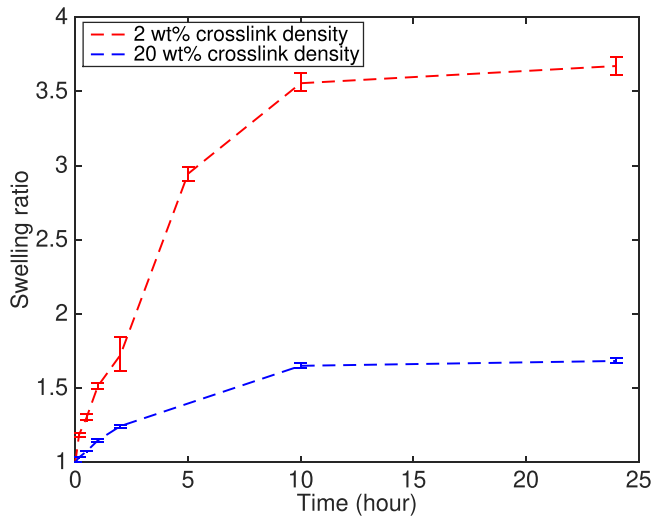


FIG. 1. The swelling ratio of two polymers as a function of the immersion time.

calculated as

$$\begin{aligned}\sigma_i &= \frac{1}{\lambda_1 \lambda_2 \lambda_3} \lambda_i \frac{\partial \widehat{\Psi}}{\partial \lambda_i} \\ &= \frac{1}{\lambda_1 \lambda_2 \lambda_3} G^{\text{eq}} (\lambda_i^2 - 1) \\ &\quad + \frac{1}{\lambda_1 \lambda_2 \lambda_3} \sum_j G_j^{\text{neq}} ((\lambda_{ji}^e)^2 - 1) - p, \\ \mu &= \frac{\partial \widehat{\Psi}}{\partial C_s} \\ &= k_B T (\ln(1 - \phi) + \phi + \chi \phi^2) + p \Omega.\end{aligned}\quad (3)$$

Following the work of Chester [30], the evolution equation of viscous stretch is represented as

$$\frac{\dot{\lambda}_{ji}^v}{\lambda_{ji}^v} = \frac{M_{ji}}{2\nu_j}, \quad (4)$$

where $M_{ji} = G_j^{\text{neq}} ((\lambda_{ji}^e)^2 - 1)$ is the Mandel stress and ν_j is the viscosity of the j th relaxation process.

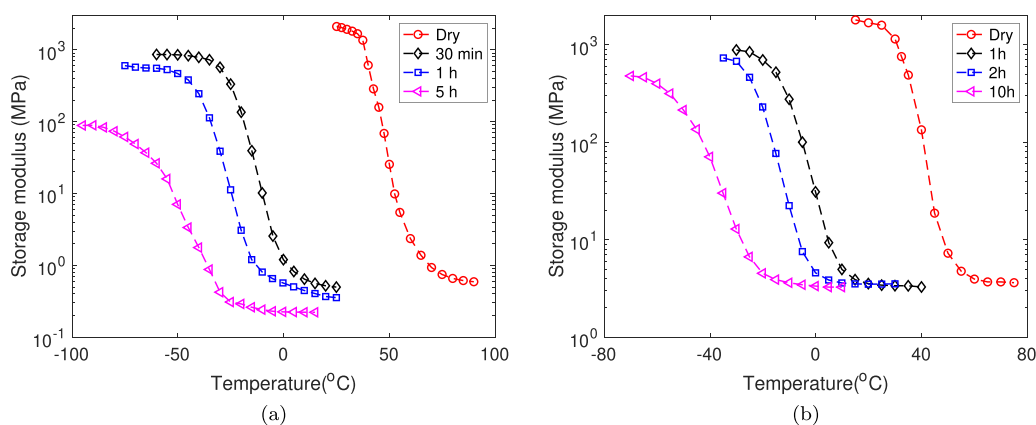


FIG. 2. The storage modulus measured at a frequency of 1 Hz for swollen gels with (a) 2 wt% cross-link density and (b) 20 wt% cross-link density.

In this work, we investigate the mechanical properties of partial swollen gels. Based on the experimental setup, we make the following assumptions. The gels have been swollen isotropically with the stretch ratio λ_s^0 in each principal direction. Before applying the mechanical deformation, the viscous stretch ratio has reached the equilibrium state $\lambda_{ji}^v = \lambda_s^0$. This assumption is reasonable since the partially swollen gels are in the equilibrium rubbery state at room temperature as shown in the later part of the paper. The swollen gel is then subjected to a uniaxial loading deformation with $\lambda_{m1} = \lambda_m(t)$ in the principal direction with $i = 1$. Due to the symmetry, the responses in the other two principal directions are the same. Since we assume the mechanical loading does not induce volumetric change, $\lambda_{m2} = \lambda_{m3} = 1/\sqrt{\lambda_m(t)}$. The elastic and viscous stretches in the principal directions have the relationship as $\lambda_s \lambda_m = \lambda_{j1}^e \lambda_{j1}^v$ and $\lambda_s / \sqrt{\lambda_m} = \lambda_{j2}^e \lambda_{j2}^v$. The corresponding true stress can be represented as

$$\begin{aligned}\sigma_1 &= \frac{1}{\lambda_s^3} G^{\text{eq}} ((\lambda_s^0 \lambda_m)^2 - 1) + \frac{1}{\lambda_s^3} \sum_j G_j^{\text{neq}} ((\lambda_{j1}^e)^2 - 1) - p, \\ \sigma_2 &= \frac{1}{\lambda_s^3} G^{\text{eq}} \left(\left(\frac{\lambda_s^0}{\sqrt{\lambda_m}} \right)^2 - 1 \right) \\ &\quad + \frac{1}{\lambda_s^3} \sum_j G_j^{\text{neq}} ((\lambda_{j2}^e)^2 - 1) - p.\end{aligned}\quad (5)$$

The evolution equation for the viscous stretch of Eq. (4) can be rewritten as

$$\frac{\dot{\lambda}_{j1}^v}{\lambda_{j1}^v} = \frac{(\lambda_{j1}^e)^2 - 1}{2\tau_j}, \quad \frac{\dot{\lambda}_{j2}^v}{\lambda_{j2}^v} = \frac{(\lambda_{j2}^e)^2 - 1}{2\tau_j}, \quad (6)$$

where $\tau_j = \nu_j / G_j^{\text{neq}}$ is the relaxation time.

The above equations can be further linearized if the applied deformation is small. The applied mechanical strain in the loading direction can be represented as $\epsilon_m = \ln \lambda_m$. Correspondingly, the mechanical strain in the other two principal directions can be estimated as $-0.5\epsilon_m$. The elastic and viscous strains can be defined as $\epsilon_{j1}^e = \ln \lambda_{j1}^e$ and $\epsilon_{j1}^v = \ln \lambda_{j1}^v$. Similarly, the corresponding elastic and viscous strains in the other two directions can be represented as $\epsilon_{j2}^e = \ln \lambda_{j2}^e$ and

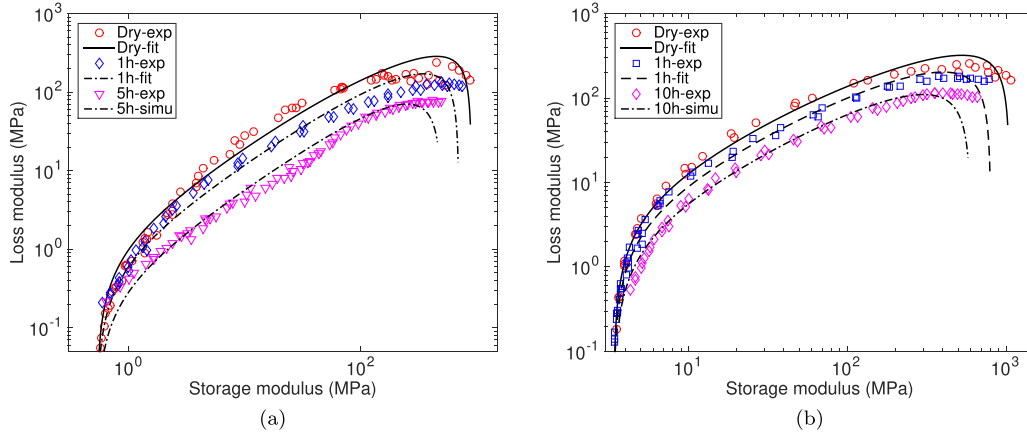


FIG. 3. The loss modulus as a function of storage modulus (Cole-Cole plot) of the swollen gels with (a) 2 wt% cross-link density and (b) 20 wt% cross-link density.

$\epsilon_{j2}^v = \ln \lambda_{j2}^v$. Considering that the value of λ_{ji}^e is close to 1 and the value of λ_{ji}^v is close to λ_s^0 , the elastic and viscous strains can be represented as $\lambda_{ji}^e = 1 + \epsilon_{ji}^e$ and $\lambda_{ji}^v = \lambda_s^0(1 + \epsilon_{ji}^v)$. Thus, Eq. (6) can be written as

$$\dot{\epsilon}_{j1}^v = \frac{\epsilon_{j1}^e}{\tau_j}, \quad \dot{\epsilon}_{j2}^v = \frac{\epsilon_{j2}^e}{\tau_j}. \quad (7)$$

From Eq. (7), the following relationship can be obtained,

$$\dot{\epsilon}_{j1}^v + 2\dot{\epsilon}_{j2}^v = \frac{\epsilon_{j1}^e + 2\epsilon_{j2}^e}{\tau_j}. \quad (8)$$

Considering the volume incompressible by the mechanical deformation, we have $\epsilon_{j1}^e + 2\epsilon_{j2}^e + \epsilon_{j1}^v + 2\epsilon_{j2}^v = 0$ and the initial state $\epsilon_{j1}^e(t=0) + 2\epsilon_{j2}^e(t=0) = 0$. Combining Eq. (8) and the above conditions, we can obtain $\epsilon_{j2}^e = -0.5\epsilon_{j1}^e$ and $\epsilon_{j2}^v = -0.5\epsilon_{j1}^v$.

Thus, Eq. (5) can be written as

$$\begin{aligned} \sigma_1 &= \frac{G^{\text{eq}}}{\lambda_s^0} 2\epsilon_m + \sum_j^N \frac{G_j^{\text{neq}}}{\lambda_s^{0^3}} 2\epsilon_{j1}^e - p, \\ \sigma_2 &= -\frac{G^{\text{eq}}}{\lambda_s^0} \epsilon_m - \sum_j^N \frac{G_j^{\text{neq}}}{\lambda_s^{0^3}} \epsilon_{j1}^e - p. \end{aligned} \quad (9)$$

Since $\sigma_2 = 0$, the pressure term p can be eliminated as

$$\sigma_1 = \frac{3G^{\text{eq}}}{\lambda_s^0} \epsilon_m + \sum_j^N \frac{3G_j^{\text{neq}}}{\lambda_s^{0^3}} \epsilon_{j1}^e. \quad (10)$$

Thus, the stress response can be obtained by combining Eqs. (7) and (10). We further derive the storage modulus and loss modulus of the swollen gels. We assume a small amplitude dynamic strain $\epsilon_m = \Delta\epsilon_0 e^{i\omega t}$, where $\Delta\epsilon_0$ is the amplitude and ω is the angular frequency. The corresponding stress can be calculated using Eqs. (7) and (10) as

$$\begin{aligned} \sigma_1 &= \left(\frac{E^{\text{eq}}}{\lambda_s^0} + \sum_j^N \frac{E_j^{\text{neq}}}{\lambda_s^{0^3}} \frac{\omega^2 \tau_j^2}{1 + \omega^2 \tau_j^2} \right) \Delta\epsilon_0 e^{i\omega t} \\ &+ i \left(\sum_j^N \frac{E_j^{\text{neq}}}{\lambda_s^{0^3}} \frac{\omega \tau_j}{1 + \omega^2 \tau_j^2} \right) \Delta\epsilon_0 e^{i\omega t}, \end{aligned} \quad (11)$$

where $E^{\text{eq}} = 3G^{\text{eq}}$ and $E_j^{\text{neq}} = 3G_j^{\text{neq}}$ are the equilibrium and nonequilibrium Young's moduli.

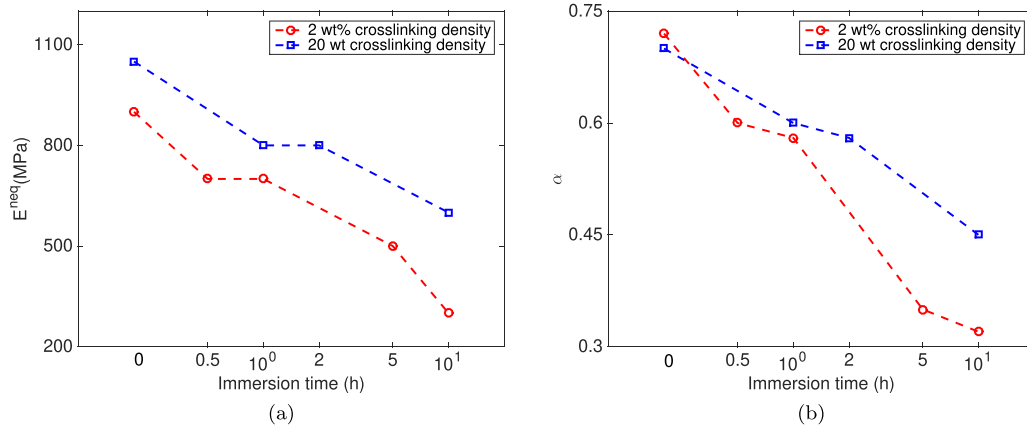


FIG. 4. The obtained parameters (a) E^{neq} and (b) α as a function of immersion time.

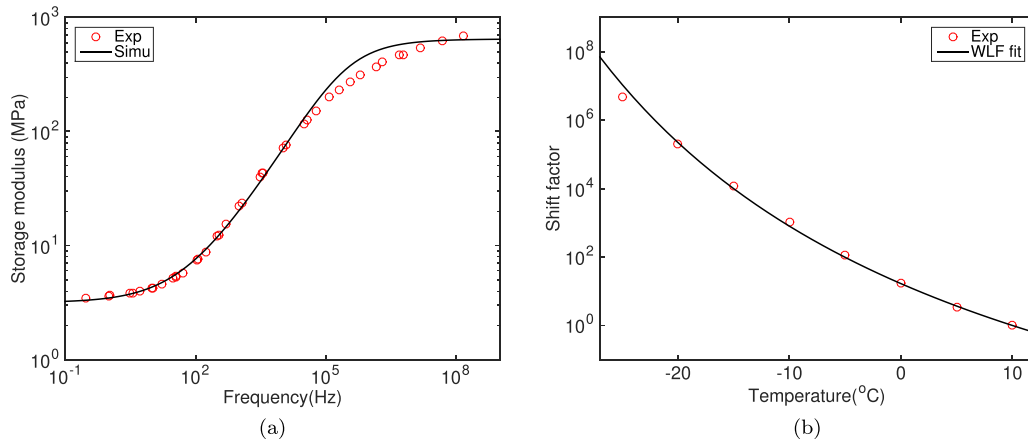


FIG. 5. For polymers with 20 wt% cross-link density and two hours immersion time: (a) the master curve of storage modulus and (b) the shift factor obtained through the time-temperature superposition principal.

Thus, the storage modulus E' and loss modulus E'' can then be obtained as

$$E' = \frac{E^{\text{eq}}}{\lambda_s^0} + \sum_j^N \frac{E_j^{\text{neq}}}{\lambda_s^{0^3}} \frac{\omega^2 \tau_j^2}{1 + \omega^2 \tau_j^2},$$

$$E'' = \sum_j^N \frac{E_j^{\text{neq}}}{\lambda_s^{0^3}} \frac{\omega \tau_j}{1 + \omega^2 \tau_j^2}. \quad (12)$$

The above results show that the equilibrium modulus of gels is related to the corresponding component of the dry polymer as $E_{\text{gel}}^{\text{eq}} = E^{\text{eq}}/\lambda_s^0$, which is consistent with the results in the literature [35]. Here we further show that the nonequilibrium modulus of gels and dry polymer is scaled by $1/\lambda_s^{0^3}$.

The distribution of $E_j^{\text{neq}} - \tau_j$ characterizes the viscoelastic relaxation spectrum. Alternatively, the viscoelastic relaxation spectrum can also be described by the continuous spectrum. For amorphous thermosets, one widely used model is the fractional Zener model with four parameters: the equilibrium Young's modulus E^{eq} , the nonequilibrium Young's modulus E^{neq} , the relaxation time τ , and the breadth of relaxation spectrum α . Here we extend the fractional Zener model for the swollen gels. The storage and loss modulus is represented as

$$E' = \frac{E^{\text{eq}}}{\lambda_s^0} + \frac{E^{\text{neq}}}{\lambda_s^{0^3}} \frac{(\omega\tau)^{2\alpha} + (\omega\tau)^\alpha \cos(\alpha\pi/2)}{1 + (\omega\tau)^{2\alpha} + 2(\omega\tau)^\alpha \cos(\alpha\pi/2)},$$

$$E'' = \frac{E^{\text{neq}}}{\lambda_s^{0^3}} \frac{(\omega\tau)^\alpha \sin(\alpha\pi/2)}{1 + (\omega\tau)^{2\alpha} + 2(\omega\tau)^\alpha \cos(\alpha\pi/2)}. \quad (13)$$

TABLE I. Parameters for the polymers with 2 wt% cross-link density.

Parameter	Dry	30 min	1 h	10 h
C_1^0	4.7	5.9	7.8	24.6
C_2^0 (K)	62.7	64.9	79.5	144.1
T_0 (K)	348	283	273	248
τ (s)	2.5×10^{-6}	8.0×10^{-7}	1.0×10^{-7}	3.0×10^{-10}

The above equation shows that given the mechanical properties of the dry polymer and the swollen ratio, the corresponding dynamic properties of swollen gels in the small strain condition can be obtained with the assumption that the viscoelastic relaxation spectrum remains unchanged in the presence of solvent. On the other side, if the dynamic properties of both dry polymer and swollen gels are provided, we can verify whether the viscoelastic relaxation spectrum changes or not. Based on Eq. (13), the corresponding storage modulus and loss modulus of the polymer matrix can be calculated given the corresponding measured properties of the swollen gels as

$$E_p' = E' \lambda_s^{0^3} + E^{\text{eq}}(1 - \lambda_s^{0^2}), \quad E_p'' = E'' \lambda_s^{0^3}. \quad (14)$$

IV. RESULTS AND DISCUSSIONS

The mass change was measured before the mechanical characterization, which can be used to calculate the volumetric swelling ratio $\lambda_s^3 = 1 + (m_t - m_0)\rho_p/(m_0\rho_s)$ with m_0 representing the initial weight of polymer, m_t representing the weight of the swollen gel, $\rho_p = 1.05 \text{ g/cm}^3$ representing the density of the polymer, and $\rho_s = 0.785 \text{ g/cm}^3$ representing the density of the IPA. Figure 1 shows the volumetric swelling ratio as a function of the immersion time for the two polymers. For two polymers, an equilibrium state can be achieved with an immersion time of 10 h. The equilibrium swelling ratio for polymers with 2 wt% cross-link density is 3.67, while the value for polymers with 20 wt% cross-link density is 1.68. Increasing the cross-link density can result in a larger free energy of stretching polymer chains, which further leads to a smaller swelling ratio.

TABLE II. Parameters for the polymers with 20 wt% cross-link density.

Parameter	Dry	1 h	2 h	10 h
C_1^0	5.5	9.9	7.8	8.8
C_2^0 (K)	55.8	78.3	73.8	82.3
T_0 (K)	333	288	283	263
τ (s)	1.1×10^{-5}	6.0×10^{-6}	7.0×10^{-7}	9.0×10^{-8}

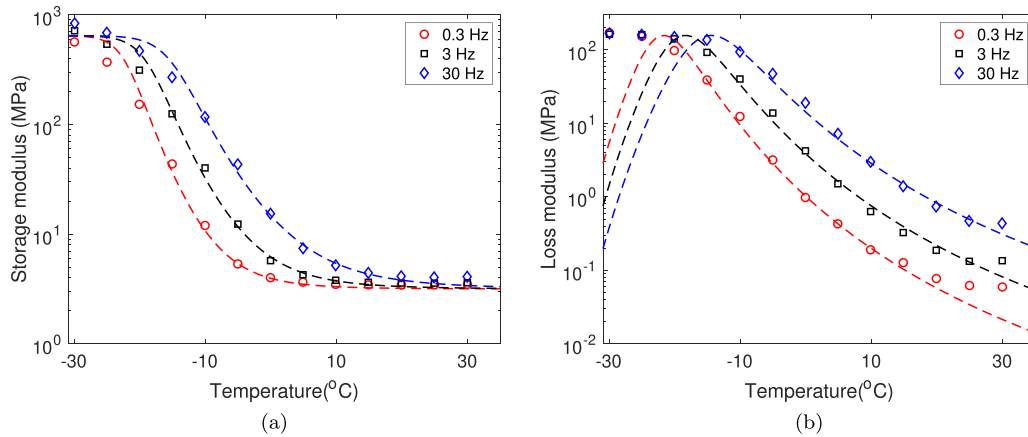


FIG. 6. Comparison between the measured and predicted (a) storage modulus and (b) loss modulus for polymers with 20 wt% cross-link density and two hours immersion time.

To obtain the glass transition region of swollen gels, the temperature-dependent storage modulus is shown in Fig. 2. The results show that the glass transition region shifts to lower temperature with increasing of the immersion time. For polymers with 2 wt% cross-link density, the onset T_g is around 40 °C while for nearly fully swollen gels (immersion time 10 h) the onset T_g is decreased to -70 °C. For polymer with 20 wt% cross-link density, the onset T_g changed from 30 °C for dry polymers to -50 °C for the fully swollen gels. It should be emphasized that even though the solvent volume fraction can occupy more than 70%, a glass transition behavior can still occur in the low temperature region in the gel systems. Classic theories, like the free volume theory and configurational entropy theory, can qualitatively explain the occurrence of glass transition. Introducing the solvent into polymer matrix can induce an increase in the free volume or configurational entropy [36], while lowering the temperature can still reduce the free volume or configurational entropy of the whole system. This provides a possible mechanism to explain the shifting of the glass transition region to lower temperatures with increasing solvent concentration.

For amorphous polymers, the viscoelastic relaxation exhibits a broad distribution of relaxation behaviors. The characteristic relaxation time typically spans several decades. Thus, a relaxation spectrum is required to fully describe the viscoelastic relaxation of amorphous polymers in the glass transition region, which can be determined using the stress relaxation tests or small strain dynamic tests. Here, we adopt the small strain dynamic tests at multiple temperatures to determine the viscoelastic relaxation spectrum. Motivated by the Cole-Cole plot to analyze the dielectric relaxation, we plot the loss modulus as a function of the storage modulus of the polymer matrix [Eq. (14)] in Fig. 3. As shown, the dynamic properties measured at different temperatures and frequencies can overlap and form a smooth curve, indicating the time-temperature superposition principal is applicable for gels. For gels with different swelling ratio, the curves do not overlap indicating that the shape of the viscoelastic relaxation spectrum of polymer matrix has been changed.

In order to quantitatively evaluate the relaxation spectrum of swollen gels, the fractional Zener model [Eq. (13) with

$\lambda_s^0 = 1$] is used to fit the Cole-Cole plot. The model totally contains four parameters, while the value of parameter τ does not influence the shape of the Cole-Cole plot. The equilibrium modulus E^{eq} and nonequilibrium modulus E^{neq} can be determined from the lower and upper bound of the storage modulus. As shown in Fig. 3, the E^{eq} is assumed to be constant for two types of gels with a value of 0.53 MPa for the polymers with 2 wt% cross-link density and 3.4 MPa for the polymers with 20 wt% cross-link density. The breadth of the relaxation spectrum has the most significant influence on the Cole-Cole plot. In general, a smaller α results in a smaller loss modulus at the same value of the storage modulus. The obtained E^{neq} and α for different swollen states are plotted in Fig. 4, showing that both values of E^{neq} and α decrease with the swelling ratio. For gels with 2 wt% cross-link density, the nonequilibrium modulus decreases from 900 MPa for the dry polymer to 300 MPa for fully swollen gels. In the presence of solvent, the breadth of relaxation spectrum is significantly expanded with a tremendous decrease in the value of α . This phenomenon has rarely been reported in the literature. Some works on copolymers [37,38] have shown that the glass transition region can be significantly expanded, which may share a similar mechanism as the observation in this work.

As shown in Fig. 3, the fractional Zener model can generally capture the features of the Cole-Cole plot. However, the model predicts a sharp decrease in the loss modulus when the storage modulus approaches its limit, which is inconsistent with the experimental observations. This is because the model assumes that the relaxation time continuously increases with decreasing temperatures. However, due to physical aging, the structure of polymers falls out of equilibrium. The relaxation time shows a limited increase with further decreasing of the temperature. Thus, for all the levels of swollen gels or dry polymers, the measured loss modulus still remains at a large value in the glassy state.

For amorphous polymers, a master curve of the dynamic properties can be constructed using the time-temperature principal. Here we use the same procedure to construct the master curves of the storage modulus for gels. Gels with 20% cross-link density and two hours immersion time ($\lambda_s^0 = 1.075$) are

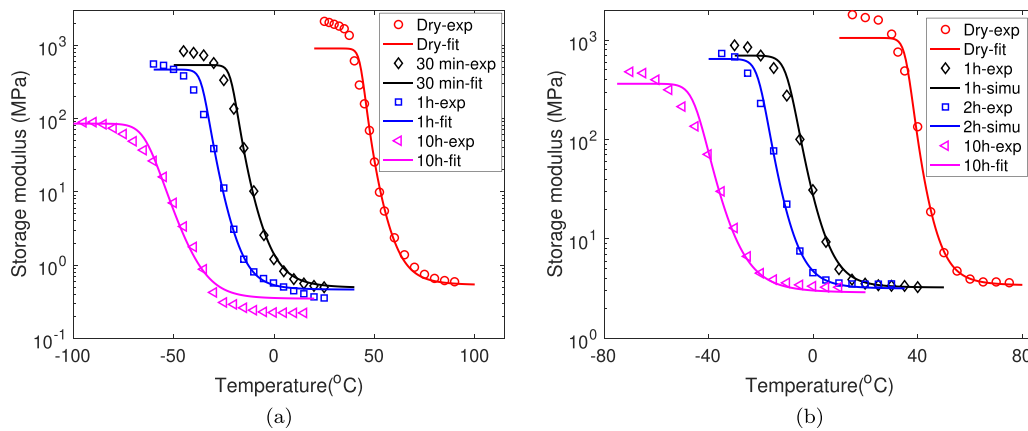


FIG. 7. Comparison between the measured and predicted temperature-dependent storage modulus for polymers with (a) 2 wt% cross-link density and (b) 20 wt% cross-link density.

provided as an example to demonstrate whether the classic methods for analyzing the rheological properties of dry polymers can also be applied for gels. Figure 5(a) shows the master curve of the storage modulus as a function of frequency while Fig. 5(b) shows the corresponding shift factor used to construct the master curve. Equation (13) is then used to fit the storage modulus. The only fitting parameter is the characteristic relaxation time τ , while the other parameters have been determined from the Cole-Cole plot. As shown, the theory can describe the obtained master curve. For amorphous polymers, the shift factor can be described by the Williams-Landel-Ferry (WLF) equation. The WLF equation can be derived based on the free volume theory or the configurational entropy theory with both widely adopted for describing the glass transition. To fit the shift factor for the swollen gels, the WLF equation with the following form is employed,

$$\log a(T) = \frac{-C_1^0(T - T_0)}{C_2^0 + T - T_0}, \quad (15)$$

where C_1^0 , C_2^0 are the WLF constants, and T_0 is the reference temperature used for constructing the master curve. Using the method shown in Ferry [39], the values of these parameters are obtained for polymers with different immersion time as listed in Tables I and II. Figure 5(b) clearly shows that the WLF equation can describe the measured shift factor.

The theory is applied to describe the storage modulus and loss modulus measured in the frequency sweep tests by combining Eqs. (13) and (15). As shown in Fig. 6, the model well reproduces the temperature-dependent and frequency-dependent dynamic properties especially in the high temperature region. In the low temperature region, the model overestimates the storage modulus. The model also predicts a sharp decrease in the loss modulus. As discussed in the previous content, these inconsistencies are due to over-

estimation of the relaxation time using the WLF equation. We also compare the measured and predicted storage modulus as a function of temperature for different specimens as shown in Fig. 7. As expected, the model can well predict the storage modulus in the glass transition region for various specimens. However, the model cannot describe the increase of storage modulus in the glassy state, which is related to fast relaxation processes and is not incorporated in the model.

V. CONCLUSION

In summary, we have investigated the glass transition behaviors of two gels with different cross-link density. It is found that glass transition still occurs in the low temperature even for heavily swollen gels. The results also show that increasing the swelling ratio leads to a lower T_g . A theory is formulated to connect the properties of polymer matrix and swollen gels. A combination of the theory and the measured dynamic properties of gels with different swelling ratios indicates that the breadth of the viscoelastic relaxation spectrum has been extended by solvents, while the glassy modulus decreases with increasing solvent concentration. The time-temperature superposition principal can still be applied to gels while the shift factor can be described by the classic WLF equation. These findings can potentially promote the fundamental understanding of the glass transition in complex material systems.

ACKNOWLEDGMENTS

The authors acknowledge the funding support from the National Natural Science Foundation of China (Grants No. 12022204 and No. 11872170) and the Fundamental Research Funds for the Central Universities (Grant No. 2021FZZX001-16).

- [1] I. Tah, S. Sengupta, S. Sastry, C. Dasgupta, and S. Karmakar, *Phys. Rev. Lett.* **121**, 085703 (2018).
 [2] C. Xia, J. Li, Y. Cao, B. Kou, X. Xiao, K. Fezzaa, T. Xiao, and Y. Wang, *Nat. Commun.* **6**, 8409 (2015).

- [3] L. Dai, C. Tian, and R. Xiao, *Int. J. Plast.* **127**, 102654 (2020).
 [4] G. W. Scherer, *Relaxation in Glass and Composites* (John Wiley and Sons, New York, 1986).

- [5] E. Donth, *The Glass Transition: Relaxation Dynamics in Liquids and Disordered Materials* (Springer-Verlag, Berlin, Heidelberg, 2013), Vol. 48.
- [6] G. Adam and J. H. Gibbs, *J. Chem. Phys.* **43**, 139 (1965).
- [7] D. Han, D. Wei, J. Yang, H.-L. Li, M.-Q. Jiang, Y.-J. Wang, L.-H. Dai, and A. Zaccone, *Phys. Rev. B* **101**, 014113 (2020).
- [8] D. R. Reichman and P. Charbonneau, *J. Stat. Mech.* (2005) P05013.
- [9] L. Janssen, *Fron. Phys.* **6**, 97 (2018).
- [10] S. K. Nandi, R. Mandal, P. J. Bhuyan, C. Dasgupta, M. Rao, and N. S. Gov, *Proc. Natl. Acad. Sci. USA* **115**, 7688 (2018).
- [11] A. Zaccone and E. M. Terentjev, *Phys. Rev. Lett.* **110**, 178002 (2013).
- [12] V. V. Palyulin, C. Ness, R. Milkus, R. M. Elder, T. W. Sirk, and A. Zaccone, *Soft. Matter* **14**, 8475 (2018).
- [13] M. Najafi, M. Habibi, R. Fokkink, W. E. Hennink, and T. Vermonden, *Soft. Matter* **17**, 2132 (2021).
- [14] R. Huang, S. Zheng, Z. Liu, and T. Y. Ng, *Inte. J. Appl. Mech.* **12**, 2050014 (2020).
- [15] Q. Ge, Z. Chen, J. Cheng, B. Zhang, Y.-F. Zhang, H. Li, X. He, C. Yuan, J. Liu, S. Magdassi *et al.*, *Sci. Adv.* **7**, eaba4261 (2021).
- [16] R. Okamoto, E. Clayton, and P. Bayly, *Phys. Med. Biol.* **56**, 6379 (2011).
- [17] B. Keshavarz, T. Divoux, S. Manneville, and G. H. McKinley, *ACS Macro Lett.* **6**, 663 (2017).
- [18] R. Tamate, K. Hashimoto, X. Li, M. Shibayama, and M. Watanabe, *Polymer* **178**, 121694 (2019).
- [19] A. Maningding and M. Azadi, *Inte. J. Appl. Mech.* **12**, 2050103 (2020).
- [20] N. Bosnjak, S. Nadimpalli, D. Okumura, and S. A. Chester, *J. Mech. Phys. Solids* **137**, 103829 (2020).
- [21] L. Dai and R. Xiao, *Inte. J. Appl. Mech.* **13**, 2150022 (2021).
- [22] P. Rao, T. Li, Z. liang Wu, W. Hong, X. Yang, H. Yu, T.-W. Wong, S. Qu, and W. Yang, *Extreme Mech. Lett.* **28**, 43 (2019).
- [23] Y. J. Wang, X. N. Zhang, Y. Song, Y. Zhao, L. Chen, F. Su, L. Li, Z. L. Wu, and Q. Zheng, *Chem. Mater.* **31**, 1430 (2019).
- [24] R. Xiao, C. Zhang, X. Gou, and W. M. Huang, *Mater. Lett.* **209**, 131 (2017).
- [25] X. Zhang, C. Du, M. Du, Q. Zheng, and Z. Wu, *Mater. Today Phys.* **15**, 100230 (2020).
- [26] A. Drozdov, C.-G. Sanporean, and J. d. C. Christiansen, *Int. J. Solids Struct.* **52**, 220 (2015).
- [27] P. J. Flory, *J. Chem. Phys.* **10**, 51 (1942).
- [28] W. Hong, X. Zhao, J. Zhou, and Z. Suo, *J. Mech. Phys. Solids* **56**, 1779 (2008).
- [29] S. A. Chester and L. Anand, *J. Mech. Phys. Solids* **58**, 1879 (2010).
- [30] S. A. Chester, *Soft Matter* **8**, 8223 (2012).
- [31] S. Reese and S. Govindjee, *Mech. Time-Depend. Mater.* **1**, 357 (1997).
- [32] P.-G. de Gennes, *J. Chem. Phys.* **55**, 572 (1971).
- [33] C. Linder, M. Tkachuk, and C. Miehe, *J. Mech. Phys. Solids* **59**, 2134 (2011).
- [34] F. J. Vernerey, R. Long, and R. Brighenti, *J. Mech. Phys. Solids* **107**, 1 (2017).
- [35] S. A. Chester and L. Anand, *J. Mech. Phys. Solids* **59**, 1978 (2011).
- [36] R. Xiao and T. D. Nguyen, *Soft. Matter* **9**, 9455 (2013).
- [37] C. Wu, C. Wei, W. Guo, and C. Wu, *J. Appl. Polym. Sci.* **109**, 2065 (2008).
- [38] L. Dai, J. Song, S. Qu, and R. Xiao, *eXPRESS Polymer Lett.* **14**, 1116 (2020).
- [39] J. D. Ferry, *Viscoelastic Properties of Polymers* (John Wiley and Sons, New York, 1980).